

Compressible Helicoidal Surface Theory for Propeller Aerodynamics and Noise

Donald B. Hanson*

Hamilton Standard, Windsor Locks, Connecticut

Acceleration potential techniques from three-dimensional thin wing theory have been generalized for propeller and prop-fan analysis. Helicoidal reference surfaces take the place of the planar surface in wing theories; otherwise the theories are equivalent. The acoustic branch of the theory, including nonlinear source terms, extends and unifies frequency domain noise theories dating back to Gutin. For aerodynamic applications, it is shown that prop-fans satisfy well-known criteria for use of linearized theory at transonic speeds by virtue of small aspect ratio and small thickness ratio. The results are in the form of integral equations for downwash as functions of thickness and steady or unsteady loading distributions. For the case of no rotation, the kernel functions reduce to well-known kernels of wing theory. The analysis, within the restrictions of linearization, treats rigorously any planform and any flight condition including the combination of subsonic roots and supersonic tips typical of prop-fans. The effects of thickness, camber, angle of attack, sweep, offset, blade interference, and tip relief are all treated without approximation.

Nomenclature

B	= number of blades
b	= chord
c_0	= ambient sound speed
FA	= face alignment, Fig. 3
g	= general source function, Eq. (13)
h	= blade thickness
h'	= chordwise slope of blade thickness
i	= $\sqrt{-1}$
$J_n, H_n^{(1)}, I_n, K_n$	= Bessel functions
K, K_L, K_T	= kernel functions
k_x	= $\bar{\omega}b/U_0$
m, n	= harmonic summation indices
ΔP	= lift pressure
p	= pressure
r, r_0	= field point and source point radii, cylindrical coordinates
$r_>, r_<$	= larger, smaller of r, r_0
r_T	= tip radius
t	= time
U, U_0	= relative velocity at field point and source point
V	= flight velocity
w	= velocity component normal to helicoid (upwash)
x, x_1	= coordinate in flight direction, see after Eq. (8)
β	= $\sqrt{1 - V^2/c^2}$
γ, ξ, r	= helicoidal field point coordinates
γ_0, ξ_0, r_0	= helicoidal source point coordinates
ϕ	= field point azimuth
$\omega, \omega_0, \bar{\omega}$	= radian frequencies
μ	= see Eq. (26)
ρ'	= density disturbance
ρ_0	= ambient density
ψ	= Fourier transform of g , see Eq. (16)
δ	= Dirac delta function

δ'	= derivative of δ
Ω	= angular velocity of propeller
Φ	= disturbance velocity potential
Ψ	= disturbance pressure potential

Introduction

OVER the past 50 years, the most powerful tools for design and analysis of airplane propellers have been a variety of lifting line methods. With these methods, induced angles of attack are calculated using three-dimensional incompressible theory and then blade section forces are determined from two-dimensional airfoil test data or two-dimensional theory. If compressibility enters the aerodynamic calculation, it is via the airfoil section characteristics. The success of this type of design method partly has been due to the fact that conventional propellers operate at subsonic tip speed, are unswept, and have only a few high aspect ratio blades. But the new prop-fans, which are currently under development for fuel conservative propulsion, pose a significantly greater challenge for analysis methods. For example, the SR-3 prop-fan design shown in Fig. 1 has eight highly swept, low aspect ratio blades. At 0.8 cruise Mach number, the section helical numbers vary between 0.84 and 1.15 from root to tip. This paper addresses the need to treat blade geometry and compressibility more realistically than is possible with lifting line methods.

The theory developed herein is intended for analysis of 1) steady performance, 2) unstalled flutter, and 3) noise radiation. Acoustic branches of the theory have been in use for several years¹⁻⁵ and agree well with test results, as shown in Fig. 2. (Further test comparisons are shown in Ref. 2.) Aerodynamic branches of the theory have not been published previously. The present paper gives a unified derivation for the aerodynamic and acoustic theory and provides the background for more applied papers to follow such as the steady performance method in Ref. 6.

Background

It is believed that the most valuable aerodynamic analysis methods for prop-fans in the near future will lie somewhere in the middle ground between the current lifting line analyses and the fully nonlinear numerical schemes also under development. The appropriate middle ground is the adaptation of thin wing theory, in which the approximation is

Received March 26, 1982; revision received Sept. 9, 1982. Copyright © American Institute of Aeronautics and Astronautics, Inc. 1982. All rights reserved.

*Principal Research Engineer, Division of United Technologies Corp., Design Department, Aircraft Systems Division. Member AIAA.

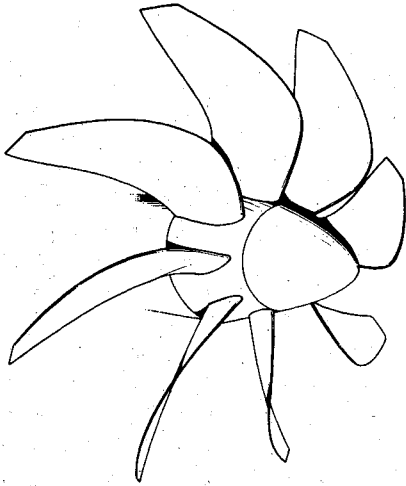


Fig. 1 Prop-fan propulsor model SR-3 designed by Hamilton Standard.

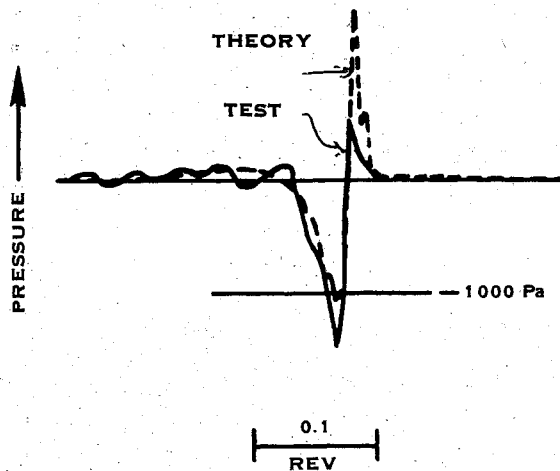


Fig. 2 Comparison of theoretical pressure waveform with data. Microphone in plane of rotation with 0.8-diameter tip clearance. Tip relative Mach number = 1.21 (Ref. 5). SR-3 prop-fan.

made that the boundary condition (of no flow through the surface) acts on a reference plane rather than on the wing upper and lower surfaces. This approximation leads to great mathematical simplifications and permits use of powerful potential field techniques. To adapt these techniques for propeller analysis, it is recognized that, in horizontal flight, each blade element travels along a helix. Thus, the natural extension of wing theory is a helicoidal surface theory. The pitch of the helicoid is determined by the flight speed and rpm so that, in the limit as $\text{rpm} \rightarrow 0$, the helicoid degenerates to a plane and the thin wing results are recovered.

Although prop-fan blade sections operate at transonic section helical speeds, the subject of linearization of the theory needs to be considered for steady and unsteady aerodynamics and for noise. For unsteady flow, Bisplinghoff and Ashley⁷ give a criterion for the use of linearized, three dimensional aerodynamics at transonic speeds.

$$k \gg \mathcal{R} \delta |\ln(\mathcal{R} \delta^{1/3})| \quad (1)$$

where $k = \omega_0 b / U$ is the reduced frequency, \mathcal{R} the aspect ratio, and δ the thickness ratio. This criterion is satisfied easily for prop-fans where a typical value of $\mathcal{R} \delta |\ln(\mathcal{R} \delta^{1/3})|$ is 0.012 and $k \approx 0.21$ at the lowest frequency of interest (once per revolution).

For steady flow the criterion for use of linearized three-dimensional aerodynamics at transonic speeds is⁷

$$\mathcal{R}^3 \delta |\ln(\mathcal{R} \delta^{1/3})|^2 \ll 1 \quad (2)$$

A typical value of $\mathcal{R}^3 \delta |\ln(\mathcal{R} \delta^{1/3})|^2$ for prop-fans is 0.023 which satisfies the steady flow criterion. (These criteria were calculated with $\mathcal{R} = 3$ and $\delta = 0.02$. For conventional propellers with $\mathcal{R} = 6$ and $\delta = 0.05$, both tests are failed completely: $k \approx 0.12$, $\mathcal{R} \delta |\ln(\mathcal{R} \delta^{1/3})| = 0.24$, $\mathcal{R}^3 \delta |\ln(\mathcal{R} \delta^{1/3})|^2 = 6.8$.) A further argument in favor of linearized aerodynamics for prop-fans is that the blades are swept to the point where the section effective Mach numbers ($M_\infty \cos \Lambda$) are subcritical. In Ref. 5 it was demonstrated with test data that linearized acoustics works well for swept blades (Fig. 2) but not so well for straight blades. Thus, for prop-fans which must be swept for noise reduction, there are good reasons to try linearization. Results for steady loading are shown in Ref. 6. In cases where local section flow is dominated by transonic effects, the linear induction theory could be coupled with two-dimensional transonic airfoil data or theory.

The recipe to be followed for calculation of the velocity potential is similar to that given in the aeroelasticity book by Bisplinghoff et al.⁸ First an expression for the pressure $p(x, r, \phi, t)$ is derived for a field point which translates (but does not rotate) with the propeller at speed V . This is given by the acoustic formulas that are used in prop-fan noise predictions. Then, for aerodynamic applications, the field point is moved to blade-fixed coordinates via the transformation $\phi = \phi_i + \Omega t$. The acceleration potential, also called the pressure potential, is written as

$$\Psi(\gamma, \xi, r, t) = -p/\rho_0 \quad (3)$$

where γ is a dimensional coordinate at constant radius in the advance helicoid and ξ a dimensional coordinate normal to γ .

The velocity potential is determined from the integral

$$\Phi(\gamma, \xi, r, t) = \frac{1}{U} \int_{-\infty}^{\gamma} \Psi\left(\lambda, \xi, r, t - \frac{\gamma - \lambda}{U}\right) d\lambda \quad (4)$$

The derivative normal to the helicoid $\partial \Phi / \partial \xi$ gives the upwash w . This results in an integral equation analogous to that of wing theory.

$$\frac{w}{U} = \int_0^T \int_0^b \frac{\Delta P}{\frac{1}{2} \rho U_0^2} K d\gamma_0 dr_0 \quad (5)$$

but with a more complicated kernel.

A similar procedure was followed by Runyan⁹ in deriving a doublet lattice method for propellers and helicopter rotors. A significant difficulty with his theory was the requirement to compute positions of all the blade elements at retarded times. In the present paper a Fourier transformation is used to eliminate this requirement at the expense of introducing a Bessel function integral that must be done numerically. The trade-off is favorable and the resulting analytical form is tractable. In fact, the kernel function has the remarkable property that it has the same form on the subsonic and supersonic parts of the blade. There is no "patching" required at the sonic radius. The physical explanation for this is that, strictly speaking, the problem treated in subsonic; there are no "zones of silence" because each portion of a blade can send signals to every other portion, as long as the flight speed is subsonic.

The acceleration potential method with a Fourier expansion was also used by Kondo¹⁰ to derive a propeller aerodynamic theory. Similar techniques have been used by Namba^{11,12} and Lordi and Homicz¹³ for ducted rotors. Kondo's theory, unlike the present work, is restricted to subsonic section speeds and steady blade loading. The far wake terms in the

steady loading kernel functions are the same but the near-field terms are quite different. In fact, Kondo's kernel is sufficiently complex that it is never written out explicitly. His only use of the full kernel is to justify use of incompressible lifting line theory for unswept, subsonic blades. No published applications of Kondo's theory have been found.

Derivation of Acceleration Potential

In this section an expression for the disturbance pressure is derived for steady or unsteady sources convected in helical paths. The starting point for the analysis is Goldstein's version of the acoustic analogy¹⁴ which gives the density disturbance $\rho' = \rho - \rho_0$ caused by surfaces in motion. The problem initially is set up with the field point and coordinate system fixed in the quiescent fluid. The propeller flies past causing a transient disturbance $\rho'(t)$. Helicoidal coordinates are defined for the sources and the thin blade approximation is made. Then the source terms are changed to a wavenumber representation via a chordwise spatial Fourier transform. The field point is then made to translate with the propeller, resulting in a harmonic density disturbance. At distances sufficiently far from the blades $c_0^2 \rho'$ can be identified as the acoustic pressure. For the steady source case, this gives the previously published acoustic theory.¹⁻⁴ Later, when the problem is linearized for aerodynamic applications, $c_0^2 \rho'$ becomes the field pressure, valid at any distance.

Goldstein's equation for the density disturbance is

$$\rho'(x, t) = -\frac{1}{c_0^2} \int_{-T}^T \int_{S(\tau)} \left(\rho_0 V_n \frac{\partial G}{\partial \tau} + f_i \frac{\partial G}{\partial y_i} \right) dS(y) d\tau + \frac{1}{c_0^2} \int_{-T}^T \int_{\nu(\tau)} T_{ij} \frac{\partial^2 G}{\partial y_i \partial y_j} dy d\tau \quad (6)$$

Quoting Goldstein, "...it is an exact result. It applies to any region $\nu(\tau)$ which is bounded by impermeable surfaces $S(\tau)$ in arbitrary motion provided the source distributions f_i and T_{ij} are localized enough to ensure convergence of the integrals." The monopole source V_n is the normal surface velocity taken to be positive away from the body. The dipole source f_i is the i th component of the force per unit area exerted by the fluid on the boundaries (sign conventions for V_n and f_i are opposite Goldstein's). The quadrupole source T_{ij} is Lighthill's stress tensor which contains the viscous and nonlinear effects. The τ integrals are over a range of source time $-T \leq \tau \leq T$ large enough to include all source times of interest. The Green's function is taken in the free space form

$$G = \frac{\delta(t - \tau - R/c_0)}{4\pi R} \quad (7)$$

where $R = |x - y|$ and x and y are observer and source locations measured from a reference point in the quiescent fluid.

For a propeller in forward flight, it is convenient to use helicoidal source coordinates

$$\gamma_0 = y_1 \quad \xi_0 = y_2 \quad r_0 = y_3 \quad (8)$$

as defined in Fig. 3. r_0 is the radius of ordinary cylindrical coordinates and γ_0 and ξ_0 are dimensional coordinates in the $r_0 = \text{constant}$ surface. γ_0 is measured backward along the advance helix in a fashion analogous to the streamwise coordinate in airfoil theories. ξ_0 is measured perpendicular to the radial and γ_0 directions. The $\xi_0 = 0$ helicoid is that surface swept out by the pitch change axis (PCA) in forward motion at speed V and rotating at angular velocity Ω . This system is convenient because only one coordinate, γ_0 , is involved in the source motion. The γ_0, ξ_0, r_0 coordinates are nonorthogonal because lines of constant γ_0 and ξ_0 are not radial. However, as shown in Appendix A of Ref. 15, this causes no additional

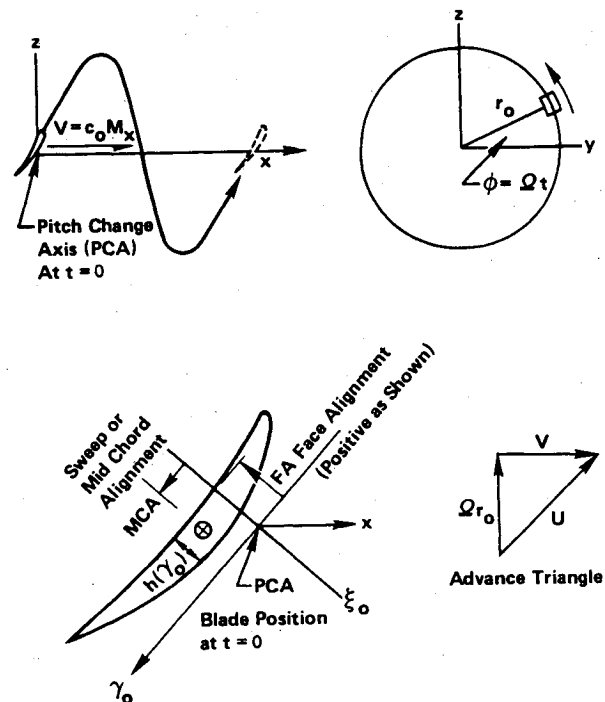


Fig. 3 Coordinates used in analysis x_0, y_0, z_0 = Cartesian source point coordinates; ξ_0, γ_0, r_0 = helicoidal source point coordinates; x, y, z = Cartesian field point coordinates; ξ, γ, r = helicoidal field point coordinates.

computational complexity and quantities like $f_i \partial G / \partial y_i$ from Eq. (6) retain their form. Various field point coordinates are used and these are listed here for reference.

- x, r, ϕ = fixed observer, x positive in flight direction
- x_1, r, ϕ = translating observer for acoustic theory, $x = x_1 + Vt$
- γ, r, ξ = blade-fixed coordinates for aerodynamic theory, corresponding to source coordinates γ_0, ξ_0, r_0 (see Fig. 3)

The distance R is found from analytic geometry to be

$$R = \left[\left(x - \frac{\Omega r_0 \xi_0}{U_0} + \frac{V \gamma_0}{U_0} \right)^2 + r^2 + r_0^2 - 2r r_0 \cos \left(\phi + \frac{\Omega \gamma_0}{U_0} + \frac{V \xi_0}{r_0 U_0} \right) \right]^{1/2} \quad (9)$$

and the blade section relative velocities at the source and field points are

$$U_0 = \sqrt{\Omega^2 r_0^2 + V^2} \quad U = \sqrt{\Omega^2 r^2 + V^2} \quad (10)$$

By transferring the boundary conditions to the helicoidal surface, the usual thin blade approximation gives $V_n = U_0 h'$ where h' is the local surface slope in the direction of motion and

$$c_0^2 \rho'(x, t) = - \int_{-\infty}^{\infty} \int_0^T \int_0^b \left[\rho_0 U_0 h' \frac{\partial G}{\partial \tau} + f_i \frac{\partial G}{\partial y_i} \right] d\gamma_0 dr_0 d\tau + \int_{-\infty}^{\infty} \int_0^{\infty} \int_{-\infty}^{\infty} \int_{-\infty}^{\infty} T_{ij} \frac{\partial^2 G}{\partial y_i \partial y_j} d\gamma_0 d\xi_0 dr_0 d\tau \quad (11)$$

where the τ integration limits have been set to ∞ assuming the integral will converge. The simplification achieved here by the thin blade approximation is that the integration limits no

longer depend on the variables. Thus, the integrations may be performed in any order. The area element $dS(y) = d\gamma_0 dr_0$ and the volume element $dy = d\gamma_0 d\xi_0 dr_0$ are established in Appendix A of Ref. 15.

Now, for convenience, the surface sources are re-expressed as volume sources via the delta function $\delta(\xi_0 + FA)$ where FA is the face alignment. Thus, for example, $h'(y, \tau) = h'(\gamma_0, r_0, \tau) \delta(\xi_0 + FA) d\xi_0$. Also, the source time and space dependence is now expressed explicitly. For a typical source, say f_i , the dependence in the blade-fixed frame would be $f_i(\gamma_0, r_0) e^{-i\omega_0 \tau}$ where $f_i(\gamma_0, r_0)$ is a complex quantity giving the amplitude and phase of the source oscillation at frequency ω_0 . However, the source is convected at speed U_0 in the $-\gamma_0$ direction. Thus, the correct space-time dependence is given by $f_i(\gamma_0 + U_0 \tau, r_0) e^{-i\omega_0 \tau}$. For the steady performance analysis, ω_0 would be set to zero, and f_i would be pure real. With these notations, Eq. (11) becomes

$$\begin{aligned} c_{\theta}^2 \rho'(x, t) = & \int_{-\infty}^{\infty} \int_0^{\infty} \int_{-\infty}^{\infty} \left\{ - \left[\rho_0 U_0 h' \frac{\partial G}{\partial \tau} \right. \right. \\ & + D \frac{\partial G}{\partial \gamma_0} + \Delta P \frac{\partial G}{\partial \xi_0} + F_r \frac{\partial G}{\partial r_0} \left. \right] \delta(\xi_0 + FA) \\ & \left. + T_{ij} \frac{\partial^2 G}{\partial y_i \partial y_j} \right\} e^{-i\omega_0 \tau} d\gamma_0 d\xi_0 dr_0 d\tau \end{aligned} \quad (12)$$

where sources on the upper and lower blade surfaces have been lumped together and D is drag force/unit area, ΔP is lift force/unit area, and F_r is radial force/unit area. Integration by parts is now used to shift the derivatives off of the Green's function and (temporarily) onto the source functions. By defining a composite source function,

$$\begin{aligned} g(\gamma_0, \xi_0, r_0) = & \left[\rho_0 U_0^2 \frac{\partial^2}{\partial \gamma_0^2} h(\gamma_0, r_0) + \frac{\partial}{\partial \gamma_0} D(\gamma_0, r_0) \right. \\ & + \frac{\partial}{\partial r_0} F_r(\gamma_0, r_0) \left. \right] \delta(\xi_0 + FA) + \Delta P(\gamma_0, r_0) \delta'(\xi_0 + FA) \\ & + \frac{\partial^2}{\partial y_i \partial y_j} T_{ij}(\gamma_0, \xi_0, r_0) \end{aligned} \quad (13)$$

Eq. (12) can now be expressed more compactly as

$$\begin{aligned} c_{\theta}^2 \rho'(x, t) = & \iiint g(\gamma_0 + U_0 \tau, \xi_0, r_0) e^{-i\omega_0 \tau} \\ & \times \frac{\delta(t - \tau - R/c_0)}{4\pi R} d\tau d\gamma_0 d\xi_0 dr_0 \end{aligned} \quad (14)$$

The τ integration is now trivial

$$\begin{aligned} c_{\theta}^2 \rho'(x, t) = & \iiint g\left(\gamma_0 + U_0 t - \frac{U_0 R}{c_0}, \xi_0, r_0\right) \\ & \times \frac{e^{-i\omega_0[t - (R/c_0)]}}{4\pi R} d\gamma_0 d\xi_0 dr_0 \end{aligned} \quad (15)$$

With $\omega_0 = 0$, this is essentially the form reported in Ref. 1.

A wavenumber representation of the source is now defined via the Fourier transform pair:

$$\psi\left(\frac{\omega}{U}, \xi_0, r_0\right) = \int_{-\infty}^{\infty} g(\gamma_0, \xi_0, r_0) \exp\left[i\frac{\omega}{U}\gamma_0\right] d\gamma_0 \quad (16)$$

$$g(\gamma_0, r_0, \xi_0) = \frac{1}{2\pi U} \int_{-\infty}^{\infty} \psi\left(\frac{\omega}{U}, \xi_0, r_0\right) \exp\left[-i\frac{\omega}{U}\gamma_0\right] d\omega \quad (17)$$

Substitution into Eq. (15) gives

$$\begin{aligned} c_{\theta}^2 \rho'(x, t) = & \iiint \frac{1}{8\pi^2 U_0 R} \int \psi\left(\frac{\omega'}{U_0}, \xi_0, r_0\right) \exp\left\{i\left[\frac{\omega' + \omega_0}{c_0} R \right. \right. \\ & \left. \left. - (\omega' + \omega_0)t - \frac{\omega' \gamma_0}{U_0}\right]\right\} d\omega' d\gamma_0 d\xi_0 dr_0 \end{aligned} \quad (18)$$

Up to this point, the analysis has treated the transient fly-by case for a fluid-fixed field point. The field point is now made to translate with the propeller at radius r and azimuth ϕ by the change of variable

$$x = x_l + Vt \quad (19)$$

which changes R in Eq. (9) to

$$\begin{aligned} R = & \left[\left(x_l + Vt - \frac{\Omega r_0 \xi_0}{U_0} + \frac{V \gamma_0}{U_0} \right)^2 + r^2 + r_0^2 \right. \\ & \left. - 2rr_0 \cos\left(\phi + \frac{\Omega \gamma_0}{U_0} + \frac{V \xi_0}{r_0 U_0}\right) \right]^{1/2} \end{aligned} \quad (20)$$

This gives the density disturbance in the translating coordinate system as

$$\rho'_l(x_l, r, \phi, t) = \rho'(x_l + Vt, r, \phi, t) \quad (21)$$

Now Weyrich's formula¹⁶

$$\frac{e^{\pm ik\sqrt{X^2 + R_0^2}}}{\sqrt{X^2 + R_0^2}} = \pm \frac{i}{2} \int_{-\infty}^{\infty} e^{\pm i\tau X} H_0^{(1)}(R_0 \sqrt{k^2 - \tau^2}) d\tau \quad (22)$$

and the Bessel function addition theorem¹⁷

$$H_0^{(1)}(K\sqrt{r^2 + r_0^2 - 2rr_0 \cos \phi}) = \sum_{n=-\infty}^{\infty} J_n(Kr_<) H_n^{(1)}(Kr_>) e^{in\phi} \quad (23)$$

(where $r_<$ is the smaller of r_0 and r and $r_>$ is the larger) are used successively to expand $\exp[i(\omega' + \omega_0)R/c_0]/R$ with the result

$$\begin{aligned} c_{\theta}^2 \rho'_l = & \iint \frac{i}{16\pi^2 U_0 V} \int \psi\left(\frac{\omega'}{U_0}, \xi_0, r_0\right) \int \sum_{n=-\infty}^{\infty} J_n \left[r_< \sqrt{\left(\frac{\omega' + \omega_0}{c_0}\right)^2 - \left(\frac{\tilde{\omega}}{V}\right)^2} \right] H_n^{(1)} \left[r_> \sqrt{\left(\frac{\omega' + \omega_0}{c_0}\right)^2 - \left(\frac{\tilde{\omega}}{V}\right)^2} \right] \\ & \times \exp\left[i\frac{\tilde{\omega}}{V} \left(x_l + Vt - \frac{\Omega r_0 \xi_0}{U_0} \right)\right] \exp\left[in\left(\phi + \frac{V \xi_0}{r_0 U_0}\right)\right] \exp[-i(\omega' + \omega_0)t] \int \exp\left[i(n\Omega - \omega' + \tilde{\omega}) \frac{\gamma_0}{U_0}\right] d\gamma_0 d\omega' d\tilde{\omega} d\xi_0 dr_0 \end{aligned} \quad (24)$$

The integral over γ_0 is the delta function $2\pi U_0 \delta(n\Omega - \omega' + \tilde{\omega})$ which facilitates the ω' integration. The result, after shifting the integration variable by $n\Omega$, is

$$\begin{aligned} c_{\theta}^2 \rho'_l(x_l, r, \phi, t) = & \frac{i}{8\pi V} \iint \sum_{n=-\infty}^{\infty} \exp\{i[n(\phi - \Omega t) - \omega_0 t]\} \exp\left[i\frac{\tilde{\omega} - n\Omega}{V} x_l\right] J_n(\mu r_<) H_n^{(1)}(\mu r_>) \int \psi\left(\frac{\tilde{\omega}}{U_0}, \xi_0, r_0\right) \\ & \times \exp\left[-i(\tilde{\omega} - n\Omega) \frac{\Omega r_0 \xi_0}{V U_0}\right] \exp\left[in \frac{V \xi_0}{r_0 U_0}\right] d\xi_0 d\tilde{\omega} dr_0 \end{aligned} \quad (25)$$

where

$$\mu = \sqrt{\left(\frac{\bar{\omega} + \omega_0}{c_0}\right)^2 - \left(\frac{\bar{\omega} - n\Omega}{V}\right)^2} \quad (26)$$

Equation (25) is the first major result of this paper. It gives the near (or far) field density disturbance measured by an observer translating, but not rotating, with the propeller. Except for the thin blade approximation, it is an exact result in that it includes all nonlinear effects and is valid at any Mach number and for any planform. Of course, it presumes that the source strengths are known. For steady sources, $\omega_0 = 0$, it can be seen that the field is steady in a coordinate system rotating with the blades at $\phi = \phi_I + \Omega t$. The reader can verify from the large argument asymptotic form of $H_n^{(1)}$ that the result contains only outgoing waves.

Acoustic Applications

In order to derive working formulas from Eq. (25) for near field noise calculations, the same procedure used for the far field theory² must be used. The details of this are left to a future paper but a simplified example is given here for the purpose of illustration. Consider the volume displacement source term from Eq. (13),

$$g_V(\gamma_0, \xi_0, r_0) = \rho_0 U_0^2 \delta(\xi_0) \frac{\partial^2}{\partial \gamma_0^2} h(\gamma_0, r_0) \quad (27)$$

where the blade face alignment FA has been set to zero. The corresponding frequency domain term from Eq. (16), after integration twice by parts, is

$$\psi_V\left(\frac{\bar{\omega}}{U_0}, \xi_0, r_0\right) = -\rho_0 U_0^2 b^2 t_b \left(\frac{\bar{\omega}}{U_0}\right)^2 \delta(\xi_0) \Psi_V\left(\frac{\bar{\omega} b}{U_0}\right) \quad (28)$$

where b is the local chord, t_b the section thickness-to-chord ratio and

$$\Psi_V\left(\frac{\bar{\omega} b}{U_0}\right) = \frac{1}{b^2 t_b} \int h(\gamma_0, r_0) \exp\left[i \frac{\bar{\omega} \gamma_0}{U_0}\right] d\gamma_0 \quad (29)$$

as in Ref. 2, is the chordwise Fourier transform of the section thickness distribution. Substitution of Eq. (28) into Eq. (25), setting $c_0^2 \rho'_I$ equal to the acoustic pressure, and extracting the n th harmonic yields

$$P_{Vn} = \frac{-i\rho_0}{8\pi V} \int_0^T b^2 t_b \int_{-\infty}^{\infty} \bar{\omega}^2 \exp\left[i \frac{\bar{\omega} - n\Omega}{V} x_I\right] J_n(\mu r_<) H_n^{(1)}(\mu r_>) \Psi_V\left(\frac{\bar{\omega} b}{U_0}\right) d\bar{\omega} dr_0 \quad (30)$$

with $\mu = \sqrt{(\bar{\omega}/c_0)^2 - (\bar{\omega} - n\Omega)^2/V^2}$ because $\omega_0 = 0$ for a steady, convected thickness source.

Equation (30) is convenient for numerical work because of the way that x_I appears. The inner integral is a Fourier transform which permits P_{Vn} to be calculated for many directivity points (values of x_I at constant r) for the same computer cost as one point by use of fast Fourier methods. Despite the appearance of a Hankel function, the JH product has no singularities. Formulas similar to Eq. (30) for steady sources have been in use at Hamilton Standard since 1977 for linear sources and since 1978 for quadrupole sources. Although the far field noise theory of Ref. 2 was originally derived from Eq. (15) (with $\omega_0 = 0$), it can also be derived from Eq. (25). The method of stationary phase can be used to evaluate the $\bar{\omega}$ integral exactly in the limit as $r \rightarrow \infty$. The result is equivalent to Eq. (28) of Ref. 2.

Derivation of Velocity Potential

For aerodynamic calculations, the quadrupole source terms do not appear to be useful. Thus, in the following, only the linear source terms (the surface terms) are retained and the linearization is completed by interpreting $c_0^2 \rho'$ as the pressure.

The field point coordinates are moved to a blade-fixed system via

$$\phi = \phi_I + \Omega t \quad (31)$$

the x_I, ϕ_I variables are changed to streamwise and normal coordinates γ and ξ via

$$x_I = \frac{\Omega r}{U} \xi - \frac{V}{U} \gamma \quad (32)$$

$$\phi_I = -\frac{V}{Ur} \xi - \frac{\Omega}{U} \gamma \quad (33)$$

and the original source representation is recovered using Eq. (16). This gives the result

$$p(\gamma, \xi, r, t) = \frac{ie^{-i\omega_0 t}}{8\pi V} \iiint g(\gamma_0, \xi_0, r_0) \sum_{n=-\infty}^{\infty} \int J_n(\mu r_<) H_n^{(1)}(\mu r_>) \exp[-i(\bar{\omega} - \omega_0)(\gamma - \gamma_0)] \\ \times \exp\left[i\left\{[\Omega r^2(\bar{\omega} - \omega_0 - n\Omega) - nV^2] \frac{\xi}{UVr} - [\Omega r_0^2(\bar{\omega} - \omega_0 - n\Omega) - nV^2] \frac{\xi_0}{U_0 V r_0}\right\}\right] d\bar{\omega} d\gamma_0 d\xi_0 dr_0 \quad (34)$$

Fortunately, the streamwise field point variable appears in a simple way so that Eqs. (3) and (4) can be applied straightforwardly to find the velocity potential.

$$\Phi(\gamma, \xi, r, t) = \frac{-ie^{-i\omega_0 t}}{8\pi\rho_0 V} \iint g(\gamma_0, \xi_0, r_0) \sum_{n=-\infty}^{\infty} \int J_n(\mu r_<) H_n^{(1)}(\mu r_>) \exp\left\{i\left[\omega_0 \frac{\gamma}{U} + \left(\frac{\bar{\omega} - \omega_0}{U_0}\right) \gamma_0\right]\right\} \\ \times \frac{1}{U} \int_{-\infty}^{\gamma} \exp\left[-i \frac{\bar{\omega} \lambda}{U}\right] d\lambda \exp\left[i\left\{\left[\Omega r^2 (\bar{\omega} - \omega_0 - n\Omega) - nV^2\right] \frac{\xi}{UVr} - \left[\Omega r_0^2 (\bar{\omega} - \omega_0 - n\Omega) - nV^2\right] \frac{\xi_0}{U_0 V r_0}\right\}\right] d\bar{\omega} d\gamma_0 d\xi_0 dr_0 \quad (35)$$

This requires evaluation of the improper λ integral, which with the proper limiting process, can be shown to be¹⁸

$$\frac{1}{U} \int_{-\infty}^{\infty} \exp\left[-i \frac{\bar{\omega}}{U} \lambda\right] d\lambda = \left[\pi \delta(\bar{\omega}) + \frac{i}{\bar{\omega}}\right] \exp\left[-i \frac{\bar{\omega}}{U} \gamma\right] \quad (36)$$

This leads to the general result

$$\Phi(\gamma, \xi, r, t) = \frac{-e^{-i\omega_0 t}}{4\pi\rho_0 V} \iint g(\gamma_0, \xi_0, r_0) \sum_{n=-\infty}^{\infty} I_n\left(\left|\frac{\omega_0 + n\Omega}{V}\right| r_<\right) K_n\left(\left|\frac{\omega_0 + n\Omega}{V}\right| r_>\right) \exp\left[i\omega_0 \left(\frac{\gamma}{U} - \frac{\gamma_0}{U_0}\right)\right] \\ \times \exp\left[-i\left\{\left[\Omega r^2 (\omega_0 + n\Omega) + nV^2\right] \frac{\xi}{UVr} - \left[\Omega r_0^2 (\omega_0 + n\Omega) + nV^2\right] \frac{\xi_0}{U_0 V r_0}\right\}\right] d\gamma_0 d\xi_0 dr_0 \\ + \frac{e^{-i\omega_0 t}}{8\pi\rho_0 V} \iint g(\gamma_0, \xi_0, r_0) \sum_{n=-\infty}^{\infty} \int \frac{1}{\bar{\omega}} J_n(\mu r_<) H_n^{(1)}(\mu r_>) \exp\left\{-i\left[(\bar{\omega} - \omega_0) \left(\frac{\gamma}{U} - \frac{\gamma_0}{U_0}\right)\right]\right\} \\ \times \exp\left[i\left\{\left[\Omega r^2 (\bar{\omega} - \omega_0 - n\Omega) - nV^2\right] \frac{\xi}{UVr} - \left[\Omega r_0^2 (\bar{\omega} - \omega_0 - n\Omega) - nV^2\right] \frac{\xi_0}{U_0 V r_0}\right\}\right] d\bar{\omega} d\gamma_0 d\xi_0 dr_0 \quad (37)$$

where the modified Bessel functions I_n and K_n came from J_n and $H_n^{(1)}$ with pure imaginary arguments according to¹⁷

$$J_n(iz_1) H_n^{(1)}(iz_2) = \frac{2}{\pi i} I_n(z_1) K_n(z_2) \quad (38)$$

Equation (37) is the major aerodynamic result of this paper. It gives the velocity potential for any linear, helically convected, steady or unsteady source. To apply the equation, the specific source of interest (ΔP in the case of flutter) is substituted for the general source term of Eq. (13) and the ξ_0 integration is performed. The upwash is found from $w = \partial\Phi/\partial\xi$ and is evaluated on the helical reference surface, as in wing theory, by passing to the limit as $\xi \rightarrow 0$.

Aerodynamic Applications

In acoustic applications of the theory, it is generally assumed that the source strengths are known. The aerodynamicist, however, does not have this luxury; his job is usually to find the blade surface pressure distribution. This is accomplished by solving an integral equation subject to the boundary condition that the flow be tangent to the blade camber surface. As with wing methods, arbitrary camber and angle of attack can be treated rigorously. The required downwash velocity, derived by differentiating Eq. (37) in the preceding section, is, in its most general form

$$w(\gamma, \xi, r, t) = \frac{ie^{-i\omega_0 t}}{4\pi\rho_0 V^2 U r} \iint g(\gamma_0, \xi_0, r_0) \sum_{n=-\infty}^{\infty} \left[\Omega r^2 (\omega_0 + n\Omega) + nV^2\right] I_n\left(\left|\frac{\omega_0 + n\Omega}{V}\right| r_<\right) K_n\left(\left|\frac{\omega_0 + n\Omega}{V}\right| r_>\right) \\ \times \exp\left\{i\left[\Omega r_0^2 (\omega_0 + n\Omega) + nV^2\right] \frac{\xi_0}{U_0 V r_0}\right\} \exp\left\{-i\left[\Omega r^2 (\omega_0 + n\Omega) + nV^2\right] \frac{\xi}{UVr}\right\} \exp\left[i\omega_0 \left(\frac{\gamma}{U} - \frac{\gamma_0}{U_0}\right)\right] d\gamma_0 d\xi_0 dr_0 \\ + \frac{ie^{-i\omega_0 t}}{8\pi\rho_0 V^2 U r} \iint g(\gamma_0, \xi_0, r_0) \sum_{n=-\infty}^{\infty} \int_{-\infty}^{\infty} \frac{1}{\bar{\omega}} \left[\Omega r^2 (\bar{\omega} - \omega_0 - n\Omega) - nV^2\right] J_n(\mu r_<) H_n^{(1)}(\mu r_>) \\ \times \exp\left\{-i\left[\Omega r_0^2 (\bar{\omega} - \omega_0 - n\Omega) - nV^2\right] \frac{\xi_0}{U_0 V r_0}\right\} \exp\left\{i\left[\Omega r^2 (\bar{\omega} - \omega_0 - n\Omega) - nV^2\right] \frac{\xi}{UVr}\right\} \\ \times \exp\left[-i(\bar{\omega} - \omega_0) \left(\frac{\gamma}{U} - \frac{\gamma_0}{U_0}\right)\right] d\bar{\omega} d\gamma_0 d\xi_0 dr_0 \quad (39)$$

The source function g is specialized in different ways for flutter and for steady performance analysis. Equation (39) applies to a one-bladed rotor; if blade interference is important, then a sum over the blades must be included.

Unstalled Flutter

For flutter analysis, it is desired to find the unsteady blade pressure distribution associated with blade motion given by $w(\gamma_0, r_0) e^{-i\omega_0 t}$, where w , in general, is complex. Therefore, the lift pressure is selected from the general source function in Eq. (13)

$$g \rightarrow \Delta P(\gamma_0, r_0) \delta'(\xi_0) \quad (40)$$

Substituting into Eq. (39), integrating by parts on ξ_0 , and then placing the control point on the $\xi = 0$ surface gives

$$\frac{w(\gamma, r)}{U} = \int_0^{r_T} \int_0^b \frac{\Delta P(\gamma_0, r_0)}{\frac{1}{2}\rho_0 U_0^2} K(\gamma, r; \gamma_0, r_0; V, \Omega; \omega_0) d\gamma_0 dr_0 \quad (41)$$

where the kernel function is

$$K = \frac{U_0}{8\pi V^3 U^2 r r_0} \lim_{\xi \rightarrow 0} \sum_{n=-\infty}^{\infty} [\Omega r^2 (\omega_0 + n\Omega) + nV^2] [\Omega r_0^2 (\omega_0 + n\Omega) + nV^2] I_n \left(\left| \frac{\omega_0 + n\Omega}{V} \right| r_{<} \right) K_n \left(\left| \frac{\omega_0 + n\Omega}{V} \right| r_{>} \right) \\ \times \exp \left\{ -i [\Omega r^2 (\omega_0 + n\Omega) + nV^2] \frac{\xi}{UVr} \right\} \exp \left[i\omega_0 \left(\frac{\gamma}{U} - \frac{\gamma_0}{U_0} \right) \right] - \frac{U_0}{16\pi V^3 U^2 r r_0} \lim_{\xi \rightarrow 0} \sum_{n=-\infty}^{\infty} \int_{-\infty}^{\infty} \frac{1}{\tilde{\omega}} [\Omega r^2 (\tilde{\omega} - \omega_0 - n\Omega) - nV^2] \\ \times [\Omega r_0^2 (\tilde{\omega} - \omega_0 - n\Omega) - nV^2] J_n(\mu r_{<}) H_n^{(1)}(\mu r_{>}) \exp \left\{ i [\Omega r^2 (\tilde{\omega} - \omega_0 - n\Omega) - nV^2] \frac{\xi}{UVr} \right\} \exp \left[-i(\tilde{\omega} - \omega_0) \left(\frac{\gamma}{U} - \frac{\gamma_0}{U_0} \right) \right] d\tilde{\omega} \quad (42)$$

and

$$\mu = \sqrt{\left(\frac{\tilde{\omega}}{c_0} \right)^2 - \left(\frac{\tilde{\omega} - \omega_0 - n\Omega}{V} \right)^2} \quad (43)$$

Equation (41) is a generalization of the unsteady wing integral equation studied by Watkins et al.¹⁹ and in the Appendix of Ref. 15 is shown to reduce to it in the limit as $\Omega \rightarrow 0$. The integral equation can be solved by the types of inversion methods used for wing analysis. The incompressible version of Eq. (41) (obtained by letting $c_0 \rightarrow \infty$), was originally derived by Tsakonas²⁰ and his co-workers at Stevens Institute.

Steady Performance

Thickness is not a primary source in wing analysis because it does not cause upwash in the wing plane. However, for a propeller, thickness will produce upwash at the helicoidal surfaces because of twist and blade interference. Moreover, for prop-fans, experience with acoustics indicates that thickness and lift sources are about equally important. These sources, therefore, are selected from the general source term in Eq. (13) so that

$$g(\gamma_0, \xi_0, r_0) = \rho_0 U_0^2 \frac{\partial^2}{\partial \gamma_0^2} h(\gamma_0, r_0) \delta(\xi_0 + FA) + \Delta P(\gamma_0, r_0) \delta'(\xi_0 + FA) \quad (44)$$

By substituting this into Eq. (39), setting $\omega_0 = 0$ and integrating by parts to remove the derivatives from the source terms, the following integral equations are found for upwash due to thickness w_T and upwash due to loading w_L

$$\frac{w_T(\gamma, r)}{U} = \int_0^{r_T} \int_0^b \frac{h(\gamma_0, r_0)}{b} K_T(\gamma, r; \gamma_0, r_0; V, \Omega) d\gamma_0 dr_0 \quad (45)$$

$$\frac{w_L(\gamma, r)}{U} = \int_0^{r_T} \int_0^b \frac{\Delta P(\gamma_0, r_0)}{\frac{1}{2}\rho_0 U_0^2} K_L(\gamma, r; \gamma_0, r_0; V, \Omega) d\gamma_0 dr_0 \quad (46)$$

In the preceding

$$K_T = \frac{-ibB}{8\pi V^2 U^2 r} \lim_{\xi \rightarrow 0} \sum_{m=-\infty}^{\infty} \int_{-\infty}^{\infty} [\Omega r^2 (\tilde{\omega} - mB\Omega) - mBV^2] \tilde{\omega} J_{mB}(\mu r_{<}) H_{mB}^{(1)}(\mu r_{>}) \\ \times \exp \left\{ i [\Omega r^2 (\tilde{\omega} - mB\Omega) - mBV^2] \frac{\xi}{UVr} \right\} \exp \left[-i\tilde{\omega} \left(\frac{\gamma}{U} - \frac{\gamma_0}{U_0} \right) \right] d\tilde{\omega} \quad (47)$$

and

$$K_L = \frac{U_0^3 B^3}{8\pi V^3 U^2 r r_0} \lim_{\xi \rightarrow 0} \sum_{m=-\infty}^{\infty} m^2 I_{mB} \left(|m| B \frac{\Omega r_{<}}{V} \right) K_{mB} \left(|m| B \frac{\Omega r_{>}}{V} \right) \exp \left[-imB \frac{U\xi}{Vr} \right] \\ - \frac{U_0 B}{16\pi V^3 U^2 r r_0} \lim_{\xi \rightarrow 0} \sum_{m=-\infty}^{\infty} \int_{-\infty}^{\infty} \frac{1}{\tilde{\omega}} [\Omega r^2 (\tilde{\omega} - mB\Omega) - mBV^2] [\Omega r_0^2 (\tilde{\omega} - mB\Omega) - mBV^2] \\ \times J_{mB}(\mu r_{<}) H_{mB}^{(1)}(\mu r_{>}) \exp \left\{ i [\Omega r^2 (\tilde{\omega} - mB\Omega) - mBV^2] \frac{\xi}{UVr} \right\} \exp \left[-i\tilde{\omega} \left(\frac{\gamma}{U} - \frac{\gamma_0}{U_0} \right) \right] d\tilde{\omega} \quad (48)$$

and now $\mu = \sqrt{(\tilde{\omega}/c_0)^2 - (\tilde{\omega} - mB\Omega)^2/V^2}$. Blade interference has been accounted for rigorously by recognizing that the periodicity in the flowfield is given by harmonics $m = nB$. The other harmonics cancel, actually simplifying the calculations for multibladed rotors. K_L is the generalization to helicoidal surfaces of the familiar wing kernel⁷

$$K_{\text{wing}} = \frac{1}{8\pi(y-y_0)^2} \left[1 + \frac{x-x_0}{\sqrt{(x-x_0)^2 + \beta^2(y-y_0)^2}} \right] \quad (49)$$

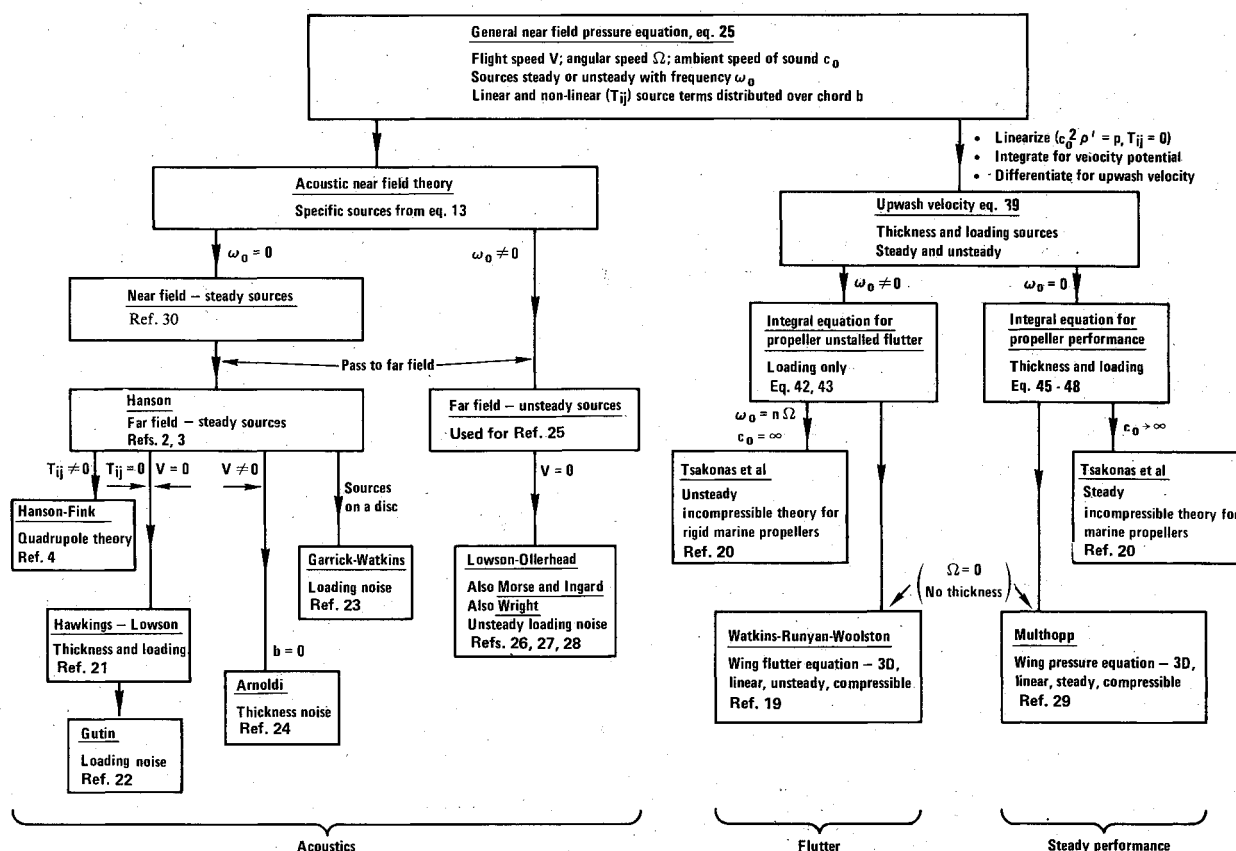


Fig. 4 Hierarchy of theoretical results.

In Appendix B of Ref. 15, it is shown that K_L reduces to K_{wing} for $B=1$ in the limit as $\Omega \rightarrow 0$, that is, as the helicoid degenerates to a planar surface. As with the wing kernel, the first term gives one half the far wake behavior and is not influenced by compressibility. The singularities of Eq. (48) enter through the infinite sum and integral. Use of Eqs. (46) and (48) for propeller performance calculations is discussed in detail in Ref. 6.

Conclusions—Relation to Previous Theories

A unified theory has been presented in which equations for acoustics, unsteady flutter, and steady performance of unshrouded propellers were derived from a single analytical model—the helicoidal lifting surface. This provides the theoretical basis for some papers already published as well as forthcoming work. As shown in Fig. 4, the general theory includes as special cases many preceding theoretical results that are familiar in propeller acoustics, ship propeller hydrodynamics, and wing aerodynamics. At the left in the figure are the frequency domain acoustic theories, which date back over 44 years. The near field, steady source theory³⁰ is used routinely at Hamilton Standard for propeller and propfan design and predictions. The far field, unsteady source theory is used to study the effect of nonuniform flowfields on propeller noise and to predict wind turbine noise caused by tower wakes.

The steady and unsteady aerodynamic branches of the theory are shown at the right in Fig. 4. Equations (42) and (47) are integral equations relating blade surface pressures and upwash velocities. These are generalizations of the wing acceleration potential theories, shown in the figure, to incorporate helicoidal reference surfaces. Propeller theory thus is given the same theoretical basis as is wing theory with its integral equations that have spawned dozens of wing methods and scores of papers over the past 30 years. Except for linearization and the thin blade approximation, the kernels of the integral equation account exactly for effects of sweep, blade interference, thickness, and three dimensionality.

References

- Hanson, D. B., "Near Field Noise of High Tip Speed Propellers in Forward Flight," AIAA Paper 76-565, 1976.
- Hanson, D. B., "Helicoidal Surface Theory for Harmonic Noise of Propellers in the Far Field," *AIAA Journal*, Vol. 18, Oct. 1980, pp. 1213-1220.
- Hanson, D. B., "Influence of Propeller Design Parameters on Far-Field Harmonic Noise in Forward Flight," *AIAA Journal*, Vol. 18, Nov. 1980, pp. 1313-1319.
- Hanson, D. B. and Fink, M. R., "The Importance of Quadrupole Sources in Prediction of Transonic Tip Speed Propeller Noise," *Journal of Sound and Vibration*, Vol. 61, Dec. 1978.
- Hanson, D. B., "The Aeroacoustics of Advanced Turbopropellers," *Mechanics of Sound Generation in Flows*, Springer-Verlag, New York, 1979, pp. 282-293.
- Hanson, D. B., "Compressible Lifting Surface Theory for Propeller Performance Calculation," Hamilton Standard, Windsor Locks, Conn., HSER 8822, April 15, 1983.
- Bisplinghoff, R. L. and Ashley, H., *Aeroelasticity*, Wiley, 1962.
- Bisplinghoff, R. L., Ashley, H., and Halfman, R. L., *Aeroelasticity*, Addison-Wesley, 1955.
- Runyan, H. L., "Unsteady Lifting Surface Theory Applied to a Propeller and Helicopter Rotor," Ph.D. Thesis, Loughborough University, Loughborough, England, 1973.
- Kondo, K., "On the Potential-Theoretical Fundamentals of the Aerodynamics of Screw Propellers at High Speed," *Journal of the Faculty of Engineering*, University of Tokyo, Vol. 25, 1957.
- Namba, M., "Lifting Surface Theory for a Rotating Subsonic or Transonic Blade Row," Aeronautical Research Council Reports and Memoranda, R&M 3740, Her Majesty's Stationery Office, London, 1974.
- Namba, M., "Three-Dimensional Analysis of Blade Forces and Sound Generation for an Annular Cascade in Distorted Flows," *Journal of Sound and Vibration*, Vol. 50, No. 4, Feb. 1977, pp. 479-508.
- Lordi, J. A. and Homicz, G. F., "Linearized Analysis of the Three-Dimensional Compressible Flow through a Rotating Annular Blade Row," *Journal of Fluid Mechanics*, Vol. 103, Feb. 1981, pp. 413-442.
- Goldstein, M. E., *Aeroacoustics*, McGraw-Hill, New York, 1976.

¹⁵Hanson, D. B., "Compressible Helicoidal Surface Theory for Propeller Aerodynamics and Noise," Hamilton Standard, Windsor Locks, Conn., HSER 8201, Sept. 29, 1981.

¹⁶Magnus, W. and Oberhettinger, F., *Formulas and Theorems for the Functions of Mathematical Physics*, Chelsea Publishing Co., New York, 1954.

¹⁷Gradshteyn, I. S. and Ryzhik, I. M., *Tables of Integrals, Series, and Products*, Academic Press, 1965.

¹⁸Champeney, D. C., *Fourier Transform and their Physical Applications*, Academic Press, London, 1973.

¹⁹Watkins, C. E., Runyan, H. L., and Woolston, D. S., "On the Kernel Function of the Integral Equation Relating Lift and Downwash Distributions of Oscillating Finite Wings in Subsonic Flow," NACA 1234, 1955.

²⁰Tsakonas, S., "Propeller Blade Pressure Distribution due to Loading and Thickness Effects," *Journal of Ship Research*, Vol. 23, June 1979, pp. 89-107.

²¹Hawkings, D. L. and Lowson, M. V., "Theory of Open Supersonic Rotor Noise," *Journal of Sound and Vibration*, Vol. 36, No. 1, Sept. 1974, pp. 1-20.

²²Gutin, L., "On the Sound Field of a Rotating Propeller," translated in NACA TM 1195, 1938.

²³Garrick, I. E. and Watkins, C. E., "A Theoretical Study of the Effect of Forward Speed on the Free-Space Sound-Pressure Field Around Propellers," NACA TR 1198, 1953.

²⁴Arnoldi, R. A., "Propeller Noise Caused by Blade Thickness," United Aircraft Research Dept., East Hartford, Conn., Rept. R-0896-1, 1956.

²⁵Metzger, F. B. and Klatte, R. J., "Status Report on Downwind Rotor Horizontal Axis Wind Turbine Noise Prediction," NASA CP 2185, Feb. 1981.

²⁶Lowson, M. V. and Ollerhead, J. B., "A Theoretical Study of Helicopter Rotor Noise," *Journal of Sound and Vibration*, Vol. 9, No. 2, March 1969, pp. 197-222.

²⁷Morse, P. M. and Ingard, K. U., *Theoretical Acoustics*, McGraw-Hill, New York, 1968.

²⁸Wright, S. E., "Discrete Radiation from Rotating Periodic Sources," *Journal of Sound and Vibration*, Vol. 17, No. 4, Aug. 1971, pp. 437-498.

²⁹Multhopp, H., "Methods for Calculating Lift Distribution of Wings (Subsonic Lifting Surface Theory)," British Aeronautical Research Council Reports and Memoranda 2884, 1953.

³⁰Hanson, D. B., "Near-Field Frequency-Domain Theory for Propeller Noise," AIAA Paper 83-0688, 1983.

From the AIAA Progress in Astronautics and Aeronautics Series . . .

GASDYNAMICS OF DETONATIONS AND EXPLOSIONS—v. 75 and COMBUSTION IN REACTIVE SYSTEMS—v. 76

*Edited by J. Ray Bowen, University of Wisconsin,
N. Manson, Université de Poitiers,
A. K. Oppenheim, University of California,
and R. I. Soloukhin, BSSR Academy of Sciences*

The papers in Volumes 75 and 76 of this Series comprise, on a selective basis, the revised and edited manuscripts of the presentations made at the 7th International Colloquium on Gasdynamics of Explosions and Reactive Systems, held in Göttingen, Germany, in August 1979. In the general field of combustion and flames, the phenomena of explosions and detonations involve some of the most complex processes ever to challenge the combustion scientist or gasdynamicist, simply for the reason that *both* gasdynamics and chemical reaction kinetics occur in an interactive manner in a very short time.

It has been only in the past two decades or so that research in the field of explosion phenomena has made substantial progress, largely due to advances in fast-response solid-state instrumentation for diagnostic experimentation and high-capacity electronic digital computers for carrying out complex theoretical studies. As the pace of such explosion research quickened, it became evident to research scientists on a broad international scale that it would be desirable to hold a regular series of international conferences devoted specifically to this aspect of combustion science (which might equally be called a special aspect of fluid-mechanical science). As the series continued to develop over the years, the topics included such special phenomena as liquid- and solid-phase explosions, initiation and ignition, nonequilibrium processes, turbulence effects, propagation of explosive waves, the detailed gasdynamic structure of detonation waves, and so on. These topics, as well as others, are included in the present two volumes. Volume 75, *Gasdynamics of Detonations and Explosions*, covers wall and confinement effects, liquid- and solid-phase phenomena, and cellular structure of detonations; Volume 76, *Combustion in Reactive Systems*, covers nonequilibrium processes, ignition, turbulence, propagation phenomena, and detailed kinetic modeling. The two volumes are recommended to the attention not only of combustion scientists in general but also to those concerned with the evolving interdisciplinary field of reactive gasdynamics.

Volume 75—468 pp., 6 × 9, illus., \$30.00 Mem., \$45.00 List
Volume 76—688 pp., 6 × 9, illus., \$30.00 Mem., \$45.00 List
Set—\$60.00 Mem., \$75.00 List

TO ORDER WRITE: Publications Dept., AIAA, 1290 Avenue of the Americas, New York, N. Y. 10104